

Final Draft
of the original manuscript:

Barkhordarian, A.; Storch, H.v.; Zorita, E.:
**Anthropogenic forcing is a plausible explanation for the observed
surface specific humidity trends over the Mediterranean area**
In: Geophysical Research Letters (2012) AGU

DOI: 10.1029/2012GL053026

1 Anthropogenic forcing is a plausible explanation for
2 the observed surface specific humidity trends over
3 the Mediterranean area

A. Barkhordarian,¹ H. von Storch^{1,2} E. Zorita¹

A. Barkhordarian, Institute for Coastal Research, Helmholtz-Zentrum Geesthacht, Max-Planck-Strasse 1, D-21502 Geesthacht, Germany (armin.h.barkhordarian@hzg.de)

H. von Storch, KlimaCampus Hamburg, Hamburg

E. Zorita, Institute for Coastal Research, Helmholtz-Zentrum Geesthacht, Max-Planck-Strasse 1, D-21502 Geesthacht, Germany

¹Institute for Coastal Research,
Helmholtz-Zentrum Geesthacht

²KlimaCampus Hamburg

4 We investigate whether the observed surface specific humidity (q) trends
5 over the Mediterranean region in the period 1974-2003 are consistent with
6 what climate models (CMIP3, CMIP5) simulate as response of q to anthro-
7 pogenic forcing (Greenhouse gas and sulphate aerosols). The natural (inter-
8 nal) variability is estimated using 6,000-year of pre-industrial control sim-
9 ulations. With the exception of winter, the increases in annual and seasonal
10 q over this region are very unlikely (with less than 1% chance) due to nat-
11 ural (internal) variability or natural forcing alone. Using several climate mod-
12 els and ensemble means, we demonstrate that the large-scale component (spatial-
13 mean trend) of the anthropogenic forcing is detectable (at 1% level) in the
14 annual and seasonal trends of q (except winter). However, the smaller-scale
15 component (spatial anomalies about the mean trend) of anthropogenic sig-
16 nal is detectable only in warm seasons (spring and summer). We further show
17 that the spread of projected trends based on A1B scenario derived from 13
18 CMIP3 models encompasses the observed trend of area-averaged q . This may
19 have important implications for the extreme precipitation, potential inten-
20 sity of cyclones and surface hydrology over the Mediterranean region.

1. Introduction

21 We here examine to what extent the observed climate trends in the Mediterranean region
22 are already an indication of the conditions described by the climate change scenarios (A1B)
23 at the end of this century. The approach used here has been earlier applied to near-surface
24 temperature [Barkhordarian et al., 2012], precipitation (Barkhordarian et al., revised) and
25 mean sea level pressure [Barkhordarian, 2012]. In the present study we investigate the
26 surface specific humidity (q) trends, which is the principal source for free-troposphere
27 water vapor and has important implications for earth radiation and energy budget and
28 therefore climate sensitivity (Willett et al. [2010] and references therein). It is also one of
29 the key variables in the hydrological cycle and in a possible intensification of precipitation
30 extremes [Allen and Ingram, 2002]. On global scale, near-surface q has been found to have
31 increased significantly by 0.07 g/Kg per decade over the time period 1973-2003 parallel to
32 rising temperature (T), with relative humidity remaining approximately constant (Willett
33 et al. [2008]). The spread of 20th century runs of CMIP3 models encapsulates the observed
34 changes (1974-1999) in the global mean, Northern Hemisphere extratropical mean (20°N
35 - 70°N) and tropical mean [Willett et al., 2010]. Large scale averages over all seasons
36 show the greatest q increase in the extratropical Northern Hemisphere, coincident with
37 the largest increase in T [Willett et al., 2010]. At the global scale the rise in surface q is
38 attributable mainly to anthropogenic GHG forcing [Willett et al., 2007]. However, regional
39 feedbacks and local forcings can lead to very different climate changes in different parts of
40 the world. Successful adaptation will necessitate increased understating of such regional
41 differences [Stott et al., 2010]. Here we analyze changes of q over the Mediterranean

42 region, among the regions likely to experience major climatic changes in the 21st century
43 as a result of the global increase in GHG concentrations [Giorgi , 2006]. Over the southern
44 European land area that is part of the Mediterranean region, moistening (1973-1999) is
45 found to be very close to the Clausius-Clapeyron scaling of saturated specific humidity
46 ($\sim 7\% K^{-1}$) and high correlations (0.85) are found between q and T [Willett et al., 2010].
47 In this study we investigate for the first time whether the observed trends in q in the
48 Mediterranean are consistent with climate change projections.

1.1. Data and Method

49 The Mediterranean area is defined here as the region from $30^{\circ}N$ to $55^{\circ}N$ and $10^{\circ}W$
50 to $40^{\circ}E$. Observed humidity data are from HadCRUH [Willett et al., 2008]: a quality
51 controlled and homogenized land and marine monthly mean anomaly 5° by 5° gridded data
52 set of surface specific humidity (q) available for the period 1973-2003. Global simulations
53 with coupled AOGCMs, provided through the WCRP CMIP3 [Meehl et al., 2007] and
54 CMIP5 [Taylor et al., 2012] are used to estimate the response of humidity to different
55 forcing (Supplementary Tables 1 and 2).

56 We follow the same approach as presented in [Barkhordarian et al., 2012]. In the first
57 step we assess whether the observed changes in q is compatible with an undisturbed
58 stationary climate and, if not, whether they are consistent with the modelled response to
59 anthropogenic and natural forcing. Comparison is carried out using un-centred correlation
60 statistics (Supplementary Eq.1). We also use un-centred and centred regression indices
61 (Supplementary Eqs. 2 and 3), which, unlike the correlation statistics, also includes
62 information about the relative magnitude of the observed and model simulated trend

63 patterns. The un-centred statistic measures the similarity of two patterns without removal
64 of the spatial mean, whereas the centred statistic refers to the similarity of deviation
65 patterns where the spatial mean has been subtracted [Santer et al., 1995].

66 The response to external forcing is defined either as the simulated trends in the observa-
67 tional period or as the trend simulated in future climate simulations. On the one hand we
68 use transient simulations derived from CMIP3 and CMIP5 archive over the period 1974
69 to 2003. We consider 3 groups of simulations. One group (GS) includes 11 simulations
70 conducted with 6 models forced with estimates of historical anthropogenic forcing only,
71 including greenhouse gases and sulphate aerosols. A second group (GHG) includes 24
72 simulations conducted with 7 models forced with historical well-mixed greenhouse gases.
73 A third group (NAT) includes 24 simulations conducted with 7 models forced with nat-
74 ural external forcing only; including volcanic aerosols and solar irradiance change. In the
75 multi-model ensembles mean of 7 models (24 GHG (NAT) simulations), the internal vari-
76 ability is reduced by about 90 percent, which leads to increasing the signal-to-noise ratio
77 in estimated signal patterns (Supplementary material). On the other hand, we use time-
78 slice climate change experiments and define the anthropogenic climate change signal (GS)
79 as the difference between the last decades of the 21st century (2071-2100, SRES A1B
80 scenario) and the reference climatology (1961-1990). We assume a linear development in
81 multi-decadal running means from 1961-2100 and the resulting signal is scaled to change
82 per year [Bhend and von Storch, 2008] (For details see supplementary Sect 1 and Table
83 2).

2. Results

2.1. Detection of externally forced changes

84 Observations show an upward trend in q in all seasons over the Mediterranean region,
85 with maximum increase in summer and minimum in winter (Fig. 1). The area mean q
86 increases by 0.04, 0.12, 0.29 and 0.13 g/Kg per decade over the period 1974-2003 in DJF,
87 MAM, JJA and SON, respectively. In contrast to specific humidity, relative humidity
88 remains approximately constant. The observed record shows a -0.1, -0.5, -0.5 and +0.03
89 %/decade changes in DJF, MAM, JJA and SON, respectively, which could be solely
90 explained by internal variability (with 1% risk of error). High positive time correlations
91 between the observed surface temperature (HadCRUT3v; Brohan et al. [2006]) and surface
92 humidity changes, correlation coefficient being +0.77, +0.92, +0.94 and +0.90 in DJF,
93 MAM, JJA and SON, respectively, is suggesting that temperature (T) and humidity (q)
94 are acting in concert. This is also suggested by Peterson et al. [2011], who indicates that
95 the ratio of latent and sensible heat content of surface atmosphere energy is positive over
96 the Mediterranean land area, pointing to the concert behavior of q and T . Following the
97 Clausius-Clapeyron relation, changes in q with increasing T should be largest in warm
98 seasons if RH remains approximately constant. This is consistent with finding maximum
99 trend of q in summer and higher T - q correlation in warm seasons. Furthermore, in low
100 latitudes and warm seasons, where the mean temperature is warmest, latent heat is the
101 dominant component in the total atmospheric energy budget at surface [Peterson et al.,
102 2011], which leads to faster increase in q with changing temperature.

103 The increase in q is pronounced throughout the region, although small areas of decreas-
104 ing q are notable in DJF and MAM (See Supplementary Fig. 1). Increasing trends in

105 q have been observed and also simulated in response to GS and GHG forcing, while the
106 observed positive trends are distinct from the predicted response to natural forcing (NAT)
107 (Fig. 2). The natural response is likely dominated by the effect of volcanoes, which induce
108 a cooling for a few years after the eruptions, and which in turn decreases q [Santer et
109 al., 2007]. Over land area, where moisture sources are restricted, the response of q to GS
110 forcing are found to be somewhat smaller than over the sea where moisture supplies are
111 not limited (Supplementary Fig. 1).

112 Here, we assess whether the observed trend of q can be due to natural (internal) vari-
113 ability alone. This is achieved by testing the null hypothesis H_0 =zero trend. To do
114 so, annual and seasonal observed trends are compared with estimated natural (internal)
115 variability derived from control integrations of CMIP3 climate models, which are pre-
116 industrial control experiments with all forcing held constant. (The number of years used
117 from the control integration of each model is presented in supplementary Table 2). From
118 6,000-year control runs we draw 194 non-overlapping 30-year segments to estimate natural
119 (internal) variability of 30-year trends. Rejecting the null hypothesis (H_0) at 98% signif-
120 icant level will indicate that there is less than 1% chance (one-sided test) that natural
121 (internal) variability rather than external drivers are responsible for the observed changes.
122 The results plotted as red whiskers in Fig. 1 indicate that no single sample of 194 segments
123 yield a positive trend of specific humidity as strong as that observed during the period
124 1974-2003, in all seasons except winter. From this we conclude that it is unlikely that the
125 observed positive trends of q can be attributed to natural (internal) variability alone, and
126 thus that externally forced changes are significantly detectable (with less than 1% risk)

127 in all seasons except winter. The lack of winter season detection of a q trend is because
128 the observed trend is too small (0.04 g/kg per decade); in addition the internal variability
129 term is higher given the higher cold season temperature variance [Barkhordarian et al.,
130 2012].

131 Having established that externally forced changes are detectable in the observed record
132 of q , we determine in a second step whether these results are consistent with what climate
133 models describe as expected response to anthropogenic (GS, GHG) or natural (NAT)
134 forcing. The distribution of regression indices is assessed from fits of regression models
135 (Supplementary Eqs. 2 and 3) to 194 non-overlapping control run segments derived
136 from 6,000 year control simulations. The quantiles of the centered (R) and un-centred
137 (UR) regression indices of 194 control run segments (O_i in Supplementary Eqs. 2 and
138 3) onto the all projected and historical anthropogenic and natural climate change signal
139 patterns (P_i in Supplementary Eqs. 2 and 3) are used to test the H_d hypothesis that the
140 distribution of regression indices does not include “zero” but includes “1”. When there is
141 insufficient evidence to reject H_d , the consistency of changes to the respective forcing is
142 claimed.

143 **2.1.1. Consistency of spatially averaged observed and climate change signal** 144 **patterns**

145 In spring (MAM) the uncentered correlation (UC) between the observed trend pattern
146 and 13 climate change projections are in the range of [0.70, 0.84]. The correlation with
147 the historical GS response pattern is 0.70 and with the historical GHG response pattern
148 the correlation is 0.88 (Supplementary Table 3). These correlations are larger than the

149 95th %tile distribution of correlation coefficients of 194 patterns of unforced trends with
150 anthropogenic signal patterns. However, the highest positive correlations are found in
151 summer, correlation coefficients being in the range of [0.82, 0.92] with 13 projections, 0.87
152 with the GS response pattern and 0.91 with the GHG response pattern. The correlation
153 between the anthropogenic signal patterns with the 194 patterns of unforced trends is
154 never as high as with observed trends (significant at 98% level). Also in autumn the
155 observed trend patterns show a high positive correlation with anthropogenic signal pat-
156 terns; correlations are in the range of [0.77, 0.86] with 13 projections, 0.85 with the GS
157 response pattern and 0.74 with the GHG response pattern. These coefficients are also
158 found to be larger than the 95th %tile distribution of control run correlations. Indeed
159 such correspondence can hardly be expected to occur if the effect of anthropogenic forcing
160 were not present in the observed record (with the probability of error of less than 2.5% in
161 spring and autumn, and 1% in summer). However, the observed record shows a zero or
162 negative correlation with natural-forcing-only simulations (NAT), correlations 0.0, -0.29,
163 0.0 and 0.1 in DJF, MAM, JJA and SON, respectively, indicating that the observed q
164 trends are distinct from the predicted response to natural forcing (NAT).

165 Figure 2 (left column) displays the uncentered regression indices (UR) and the 98th
166 %tile uncertainty range, derived from fits of the regression model (Supplementary Eq.2)
167 to 194 independent control run segments based on 6,000-year control integrations. As
168 shown in Fig. 2 (left column) in spring, summer and autumn the uncertainty interval
169 of uncentered regression indices (UR) does not include zero , but includes unity in the
170 case of all the 13 projections (black bars), the simulated GS signal patterns (green bars)

171 and the simulated GHG signal patterns (blue bars). Therefore, as the regression indices
172 within all the 15-anthropogenic signal patterns are significantly greater than zero and
173 compatible with a value of unity, we conclude that the large-scale component of anthro-
174 pogenic (GS, GHG) signal is detectable in the observed positive seasonal trends of surface
175 specific humidity at 98% significant level in all seasons, except winter. Natural-forcing-
176 only simulations (volcanic aerosols and solar irradiance change, NAT) display near zero
177 or negative regression indices and large uncertainty ranges in all seasons, indicating an
178 opposite response (decreasing q) to the observations. The uncertainty range derived from
179 the NAT simulations is considerably larger than the range estimated for GS or GHG
180 forcing (Fig. 2, left column). This could imply that the signal is dominated by the GHG
181 (GS) response, which makes it difficult to separate the smaller NAT contribution from
182 the internal climate variability.

183 **2.1.2. Consistency of observed and climate change signal anomaly patterns**

184 As shown in Fig. 2 (right column), when removing the area mean change and compar-
185 ing the anomaly patterns, the small-scale component (spatial anomalies about the spatial
186 mean trend) of GS signal is detectable in observed data only in 4 out of 13 projections
187 in spring, in 5 projections in summer and 3 projections in autumn. For the rest of the
188 models the regression indices are either negative or not significantly different from zero.
189 It is notable that in spring and summer the detection of the historical GHG forcing in
190 the observed record is robust against the removal of the area mean change. As shown in
191 Fig. 2 (right column) the uncertainty range of centred regression indices (R) in spring
192 and summer are inconsistent with “zero” and are also not significantly different from “1”,

193 indicating the detectability of the anomaly component of GHG forcing at 98% significant
194 level. In spring both historical GHG and NAT regression coefficients are found to be
195 inconsistent with “zero”, suggesting a detectable response to both historical GHG and
196 natural forcing (NAT). The fact that the detailed spatial signature in response to an-
197 thropogenic (GHG, GS) forcing is hard to detect in observed anomaly patterns may be
198 due to three factors. First, the influence of small-scale phenomena is not average out as
199 at spatial-mean scale. This leads to a decrease in the signal-to-noise ratio of externally
200 forced changes [Zwiers and Zhang, 2003]. Second, spatial representativeness of the obser-
201 vation together with model errors at grid-box-scale play important roles in the similarity
202 of anomaly patterns. Third, local forcing such as the emission of aerosols related to in-
203 dustry or traffic and/or forcing from land-use changes are locally more important [Stott
204 et al., 2010].

3. Conclusions

205 The influence of anthropogenic (GHG, GS) forcing is detectable in annual and seasonal
206 trends (except for winter) in the spatial-mean of q ; these annual and seasonal (except
207 in winter) increasing trends of q in the 1974-2003 over the region cannot be explained
208 by natural (internal) variability or natural forcing alone. However, the regional pattern
209 of trends (deviations from the spatial mean) contradicts the null hypothesis of natural
210 variability or natural forcing only in warm seasons (spring, summer). We further show
211 that the observed trends of q are within the range of changes described by 13 climate
212 change projections based on A1B scenario; therefore we conclude that observed upward
213 trend of surface specific humidity serves as an illustration of plausible future change in

214 this region [Barkhordarian et al., 2012]. This may have important implications for the
215 extreme precipitation [Allen and Ingram, 2002], potential intensity of cyclones, surface
216 hydrology [Gedney et al., 2006] and human heat stress Willett and Sherwood [2012].

References

- 217 Allen, M. R. and Ingram, W. J. (2002), Constraints on future changes in climate and the
218 hydrologic cycle. *Nature*, *419*, 224.
- 219 Barkhordarian, A., Bhend J. and von Storch H. (2012) Consistency of observed near
220 surface temperature trends with climate change projections over the Mediterranean
221 region, *Clim. Dyn.*, *38*,1695–1702.
- 222 Barkhordarian A. (2012) Investigating the Influence of Anthropogenic Forcing on Ob-
223 served Mean and Extreme Sea Level Pressure Trends over the Mediterranean Region.
224 *The Scientific World Journal*, doi:10.1100/2012/525303.
- 225 Bhend, J. and von Storch, H. (2008) Consistency of observed winter precipitation trends
226 in northern Europe with regional climate change projections, *Clim. Dyn.*, *31* 17–28.
- 227 Brohan P, Kennedy JJ, Harris I, Tett SFB and Jones PD (2006) Uncertainty estimates
228 in regional and global observed temperature changes: A new data set from 1850, *J.*
229 *Geophys. Res.*, *111*.
- 230 Gedney et al. (2006) Detection of a direct carbon dioxide effect in continental river runoff
231 records. *Nature*, *439*, 835–838.
- 232 Giorgi F (2006) Climate change hot-spots. *J. Geophys. Res.*, *33*,L08707.
- 233 Meehl et al. (2007), The WCRP CMIP3 multimodel dataset - A new era in climate change
234 research. *Bull. Amer. Meteor. Soc.*, *88*, 1383-1390.

- 235 Peterson et al. (2011), Observed changes in surface atmospheric energy over land. *J.*
236 *Geophys. Res.*, *38*, L16707.
- 237 Santer et al. (1995), Towards the detection and attribution of an anthropogenic effect on
238 climate. *Clim. Dyn.*, *12*, 77-100.
- 239 Santer et al. (2007), Identification of human-induced changes in atmospheric moisture
240 content. *Proceedings Of The National Academy Of Sciences Of The USA* *28*, 599–606.
- 241 Stott et al. (2010), Detection and attribution of climate change: a regional perspective.
242 *WIREs Clim Change*, *1*, 192-211. doi: 10.1002/wcc.34
- 243 Taylor, K. E., R. J. Stouffer, G. A. Meehl (2012) An Overview of CMIP5 and the experi-
244 ment design. *Bull. Amer. Meteor. Soc.*, *93*, doi:10.1175/BAMS-D-11-00094.1.
- 245 Willett et al. (2007), Attribution of observed surface humidity changes to human influence.
246 *Nature*, *449*, 710–U6.
- 247 Willett et al. (2008), Recent Changes in Surface Humidity: Development of the HadCRUH
248 Dataset. *J. Of Climate*, *21*, 5364–5383.
- 249 Willett et al. (2010), A comparison of large scale changes in surface humidity over land
250 in observations and CMIP3 general circulation models. *Environ. Res. Lett.*, *5*, 025210.
- 251 Willett, K. M. and Sherwood, S. (2012), Exceedance of heat index thresholds for 15 regions
252 under a warming climate using the wet-bulb globe temperature. *Inter. J. Of Climate*,
253 *32*, 161–177.
- 254 Zwiers FW and Zhang XB (2003) Toward regional-scale climate change detection, *J.*
255 *Clim.*, *16*, 793–797.

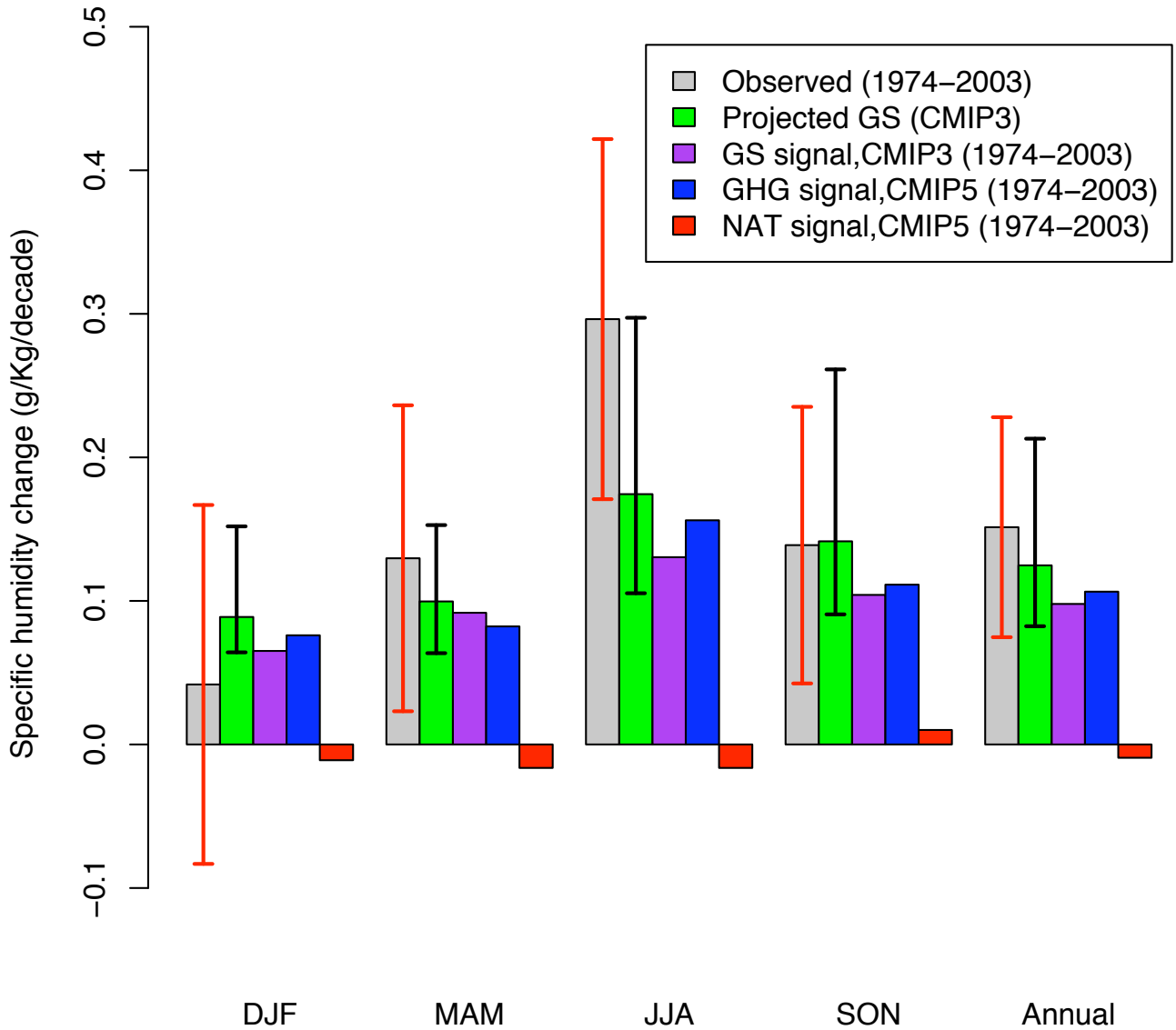


Figure 1. Observed area mean changes of surface specific humidity over the period 1974–2003 (grey bars) in comparison with 13 climate change projections estimated from time slices experiment, SRES A1B scenario (green bars), the ensembles mean of 11 historical GS forcing only simulations (purple bars), the ensembles mean of 24 historical GHG forcing only simulations (blue bars) and the ensembles mean of 24 historical natural forcing only simulations (red bars). The black whiskers indicate the spread of trends of 13 projections. The red whiskers indicate the 98th %tile uncertainty range of observed trends, derived from 6,000-year control runs. Units are

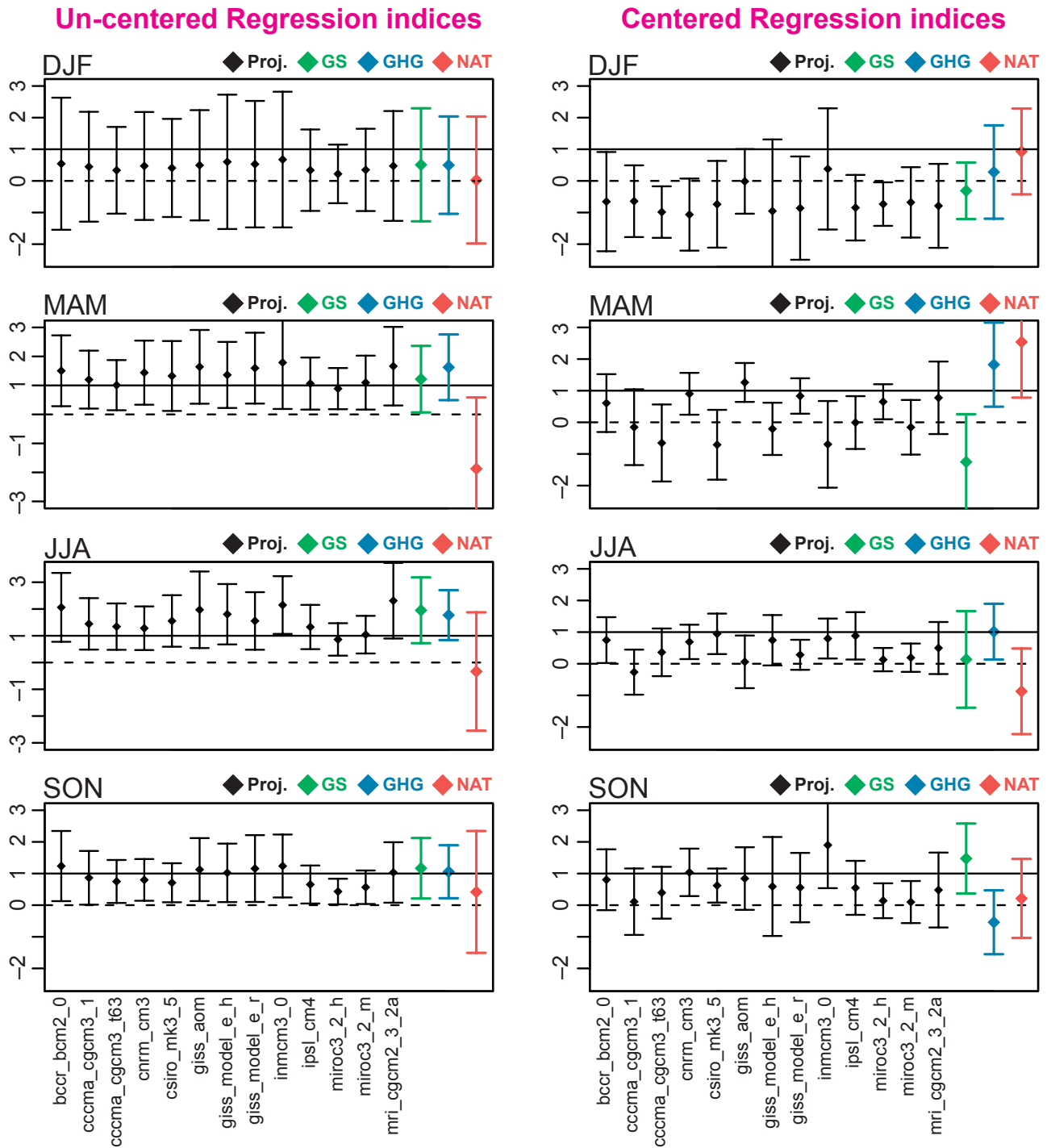


Figure 2. Seasonal un-centred regression indices (left column) and centred regression indices (right column) of observed specific humidity changes against the 13 climate change signal patterns base on SRES A1B scenario (black bars), against the simulated GS signal (green bars), the GHG signal (blue bars), and the NAT signal (red bars). The 98.4% tile uncertainty range of regression indices is derived from 6,000-year pre-industrial control simulations.